Energy and Power Management Optimization for Sequential Daily Operations in Regional Hybrid-Electric Aircraft

Emma Cassidy, Yipeng Liu,
Department of Aerospace Engineering
University Of Michigan
Ann Arbor, MI, USA
emmasmit@umich.edu;
yipenglx@umich.edu

Kathryn Kirsch,
Thermofluid Sciences
RTX Technology Research Center
East Hartford, CT, USA
kathryn.kirsch@rtx.com

Max Z. Li, and Gokcin Cinar
Department of Aerospace Engineering
University Of Michigan
Ann Arbor, MI, USA
maxzli@umich.edu;
Corresponding author: cinar@umich.edu

***Abstract*—Hybrid-Electric Aircraft (HEA) present a potential pathway to enhance propulsive efficiency and reduce operating costs in regional airline operations. This study introduces an adaptive power management strategy that optimizes allocation of electric and gas turbine engine power across sequential daily flights while addressing operational constraints such as limited gate charging durations and available ground time. HEA models are developed using physics-based and data-driven methods within the open-source Future Aircraft Sizing Tool (FAST). In contrast to prior studies that rely on fixed power splits or single-mission strategies, the proposed approach dynamically adjusts power distribution across mission phases to maximize efficiency and performance over a range of missions. Key findings indicate that sequence-optimized power management can achieve approximately a 2–3% reduction in fuel burn compared to a conventional baseline, utilizing conservative battery technology assumptions of 250 Wh/kg pack-level specific energy and a 150 kW charging power limit. The study also finds that optimizing power allocation across a full day of operations yields greater benefits than optimizing each flight independently. These results demonstrate the feasibility of HEA integration into regional airline markets, offering improved operational efficiency and cost savings while maintaining compatibility with existing fleet schedules.**

***Index Terms*—hybrid electric aircraft, electrified propulsion, power management optimization, charging strategies**

I. Introduction

Hybrid-Electric Aircraft (HEA) present a promising alternative to conventional aircraft by offering improved fuel efficiency and reduced operating costs [1], [2]. However, effective HEA design must integrate operational constraints during the early stages of aircraft design to ensure compatibility with existing airline fleets. A significant challenge arises from the current battery technology, whose specific energy (0.2-0.25 kWh/kg) is nearly 50 times lower than that of jet fuel (11.9 kWh/kg). This limitation necessitates an optimization-focused design approach that identifies the most effective use cases and operational strategies.

This work was supported by RTX under the Aircraft Design for Fleet Operations project.

The regional jet market is particularly promising for HEA integration due to its shorter-range missions, which align with moderate battery use [3]–[5]. Nonetheless, replacing conventional aircraft with HEA on regional routes may incur higher costs for airlines unless substantial fuel savings are achieved [6], [7]. In parallel hybrid-electric architectures, strategies that reduce engine takeoff power by incorporating brief periods of electric motor boost can decrease fuel consumption [8]. Yet, without an adaptive power management strategy, increasing the extent of electrification beyond the takeoff phase typically results in higher energy requirements, necessitating heavier batteries [1]. This increase in battery weight consequently elevates the aircraft's gross takeoff weight and further amplifies energy demands to meet performance targets. Moreover, constraints on gate charging durations, imposed to maintain conventional turnaround times, can further mitigate the benefits of enhanced hybridization [9].

Current research on power management for midsize to large HEA primarily focuses on propulsion architecture types and charge-depleting/sustaining strategies [10]–[12]. This paper exclusively examines parallel-hybrid electric, charge-depleting aircraft and concentrates on the effects of adaptive power management optimization during flight. Although sequential flight adaptive power management and charging strategies have been explored for UAVs [13]–[15], the distinct operational characteristics of regional HEA—such as larger battery capacities, higher payloads, longer ranges, and reduced operational flexibility—preclude direct application of UAV strategies. Consequently, a dedicated study on power management strategies for regional HEA is essential in the context of aircraft performance, propulsion system efficiency, and airline operations.

Previous work by the authors developed conventional and parallel-hybrid electric aircraft models based on the ERJ175LR regional jet using the Future Aircraft Sizing Tool (FAST) [9]. Analysis of regional airline route data from the Bureau of Transportation Statistics over a sequence of flights for a single tail number highlighted the impact of limited

gate time on charging feasibility. The findings revealed that hybridizing takeoff phase alone achieved approximately 2–3% fuel savings over conventional counterparts, while including climb hybridization imposed excessive battery weight, thereby resulting in higher fuel consumption than conventional aircraft. These outcomes were largely attributed to the use of a lower-fidelity engine model in the previous study. In this work, the engine model fidelity has been improved using the ICAO engine database method as detailed in [16].

The objective of this study is to develop an adaptive power management strategy for regional HEA that optimizes in-flight power distribution and ground charging across a sequence of flights. By dynamically allocating power between the electric motor and gas turbine engine during various mission phases, rather than relying on fixed power splits, the proposed strategy addresses constraints on gate charging with limited ground time. Leveraging sequential flight data, this study fills a critical gap in current HEA literature—which has predominantly focused on single-mission or constant power strategies—offering a scalable framework for integrating HEA into regional operations by reducing fuel consumption and enhancing fleet compatibility.

II. Technical Approach

This section describes the technical methods used to develop the aircraft models, implement adaptive power management and dynamic battery charging strategies, and formulate both single-mission and sequence-based optimization problems.

A. Model Development and Design Mission Profile

Both conventional ERJ175LR and the HEA models were developed and analyzed using FAST[1], which is an open-source, MATLAB-based aircraft sizing tool for designing and analyzing conventional and electrified aircraft concepts across any propulsion architecture [16]. These models were sized on the design mission based on a notional ERJ175LR mission, as illustrated in Fig. 1. Each flight segment is defined by specified airspeeds and altitudes consistent with the ERJ175 mission profile (Table I). The mission profile includes a reserve mission to determine the required fuel capacity in compliance with FAA safety regulations [17]. For further details on the ERJ175LR model development, see [9].

TABLE I
Mission Profile Assumptions.

Segment Value	Main Mission	Reserve
Takeoff TAS (m/s)	69.5	-
Climb EAS (m/s)	102.9	102.9
Cruise TAS (m/s)	231.3	128.6
Cruise Altitude (m)	10668	3048
Descent EAS (m/s)	108.0	102.9
Landing TAS (m/s)	-	83.3

The HEA model integrates a parallel-hybrid propulsion architecture, illustrated in Fig. 2, into a twin-fan aircraft, with one battery back powering both electric motors. Hybridization

[1]Aconventionalbaseline

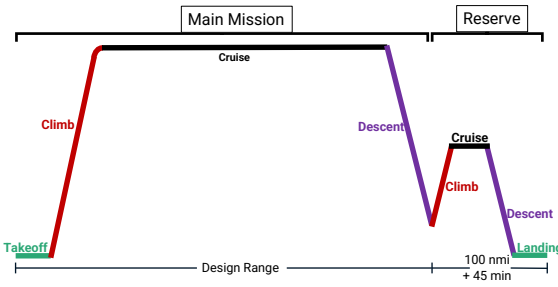

Fig. 1. Schematic of full mission profile in FAST.

is applied exclusively during takeoff and climb. The power outputs of the gas turbine engine (GT) and electric motor (EM) during climb are controlled via a throttle setting, or power code (PC), defined in 1. In off-design operations—where the aircraft design remains the same, but payload, range, and altitude targets differ from the design mission—the PC is used as an optimization variable to set the climb power output, allowing FAST to iteratively evaluate climb performance based on this control strategy. Takeoff always employs full throttle, ensuring maximum PC from all engines. Off-design missions follow the previously defined mission profile but adjust the design range and altitude to match the desired route, and all include the same reserve mission as shown in Fig. 1 and Table I.

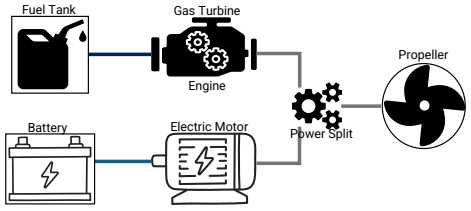

Fig. 2. Parallel-hybrid propulsion architecture.

$$P_{out} = PCP_{av}. \tag{1}$$

The following sections describe two optimization problems: one for single-mission power management and another for sequential-flight optimization that considers the effects of charging in between each flight. In both cases, FAST is treated as a black-box model, and finite difference methods are used for differentiation.

B. Single Mission Optimizer

The single-mission optimizer minimizes the block fuel burn (W_f) by adjusting the power codes for the gas turbine engine $PC_{GT,i}$ and the electric motor $PC_{EM,i}$, where i denotes the i-th point in the discretized mission profile. During takeoff, both power sources operate at full throttle, while during climb the power codes vary continuously between 0% and 100%. Critical constraints include *(i)* maintaining the State of Charge

(SOC) between 20% and 100% to ensure battery safety, *(ii)* limiting Rate of Climb (RC) to a prescribed maximum (RC_{max}) to maintain passenger comfort, *(iii)* ensuring that the required power to fly the given trajectory (P_{req}) does not exceed available power (P_{av}) from the propulsors, and *(iv)* keeping the takeoff gross weight ($TOGW$) within the maximum takeoff weight ($MTOW$) of the aircraft. The optimization problem statement is outlined below.

$$\begin{aligned} &\text{minimize} && W_f \\ &\text{by varying} && PC_{EM,i},\ PC_{GT,i}, \\ &\text{subject to} && 0\% \le PC_{EM,i} \le 100\%, \quad 0\% \le PC_{GT,i} \le 100\%, \\ & && 20\% \le SOC \le 100\%, \quad TOGW \le MTOW, \\ & && P_{\text{req},i} \le P_{\text{av},i}, \quad RC_i \le RC_{\max}. \end{aligned} \tag{2}$$

The optimization problem employs FAST with Matlab's *fmincon* function, utilizing nonlinear inequality constraints to solve for minimum fuel burn [18]. Interior-point method was chosen as the optimization algorithm due to its effectiveness in managing a large number of design variables, implementing non-linear constraints, converging even from an infeasible starting point, and locating the global minimum [19].

C. Sequence Optimizer

The sequence optimizer extends the single-mission approach to a full day of operations by optimizing the climb power codes for every mission in a flight sequence. An example sequence is illustrated in Fig. 3, which shows the design variable placements (PCs) across the discretized mission profiles and the time spent at the gate, partitioned into a fixed refueling period (first five minutes) and a subsequent charging period. The refueling time is estimated using a typical refueling truck fuel flow rate of 1000 kg/min for Jet A fuel [20].

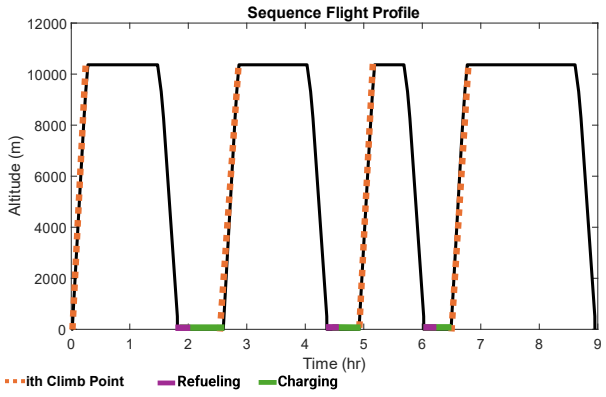

Fig. 3. Example sequence mission profile with discretized climb segment.

The sequence-based optimization problem is summarized below. Its objective is to minimize the total daily fuel burn by accounting for energy usage in each flight and adjusting the SOC for subsequent missions through the charging phase. This formulation allows the optimizer to balance energy depletion with battery state without imposing a fixed SOC threshold at the end of each mission. In this notation, k represents the mission number, ranging from 1 to n, where n is the total number of flights in the sequence.

$$\begin{aligned} &\text{minimize} && \sum_{k=1}^{n} W_{f,k} \\ &\text{by varying} && PC_{\text{EM},k,i},\ PC_{\text{GT},k,i}, \\ &\text{subject to} && 0\% \le PC_{\text{EM},k,i} \le 100\%, \quad 0\% \le PC_{\text{GT},k,i} \le 100\%, \\ & && 20\% \le SOC_k \le 100\%, \quad TOGW_k \le MTOW, \\ & && P_{\text{req},k,i} \le P_{\text{av},k,i}, \quad RC_{k,i} \le RC_{\max}. \end{aligned} \tag{3}$$

D. Updates to FAST's Battery Model

This section summarizes the modifications implemented in FAST's battery model, which now incorporates maximum discharge rate checks during battery sizing and features a more realistic charging model. The specifications for the chosen Lithium-ion battery is given in Table II.

TABLE II
RECHARGEABLE LI-ION BATTERY PARAMETERS.

Parameter	Value	Unit
Cell Nominal Voltage (V_{nom})	3.6	V
Cell Maximum Capacity ($Q_{\max}$)	3	Ah
Battery Specific Energy (e_{batt})	250	Wh/kg
System Voltage (V_{system})	223.2	V
Maximum Allowable C-rate (C_{max})	5	C
Minimum SOC threshold	20	%
Cell Internal Resistance	0.0199	Ω
Cell Maximum Extracted Voltage	4.0880	V
Number of Cells in Series (N_{ser})	62	cells
Number of Cells in Parallel (N_{par})	372	cells

1) Battery Sizing Methodology: Battery sizing critically affects the aircraft gross weight, feasibility of the hybridization strategy, and the operational flexibility. In this study, the battery pack is sized iteratively within the aircraft sizing loop based on both the energy and power requirements of the design mission. First, the desired system voltage (V_{system}) and the nominal cell voltage (V_{Nom}), determine the number of cells in series (N_{ser}):

$$N_{ser} = \frac{V_{system}}{V_{Nom}}. \tag{4}$$

During aircraft sizing, the total required battery energy (E_{req}) and the maximum required battery power (P_{max}) are computed from mission analysis. For the power-based sizing, the maximum allowable discharge current ($I_{max,cell}$) is given by

$$I_{max,cell} = C_{max} \cdot Q_{max}, \tag{5}$$

which in turn is used to determine the number of parallel cells needed for power ($N_{par,power}$):

$$N_{par,power} = \frac{P_{max}}{V_{nom} \cdot N_{ser} \cdot I_{max,cell}}. \tag{6}$$

Similarly, the number of cells in parallel based on the energy requirement, $N_{par,energy}$, is

$$N_{par,energy} = \frac{E_{req}}{V_{nom} \cdot N_{ser} \cdot Q_{max}}. \quad (7)$$

The final battery pack design uses the most restrictive (largest) value, ensuring both energy and power criteria are met:

$$N_{par} = max(N_{par,power}, N_{par,energy}). \quad (8)$$

An empirical equivalent circuit model captures the battery discharging dynamics by incorporating the open-circuit voltage (OCV) as a function of SOC, internal resistance, discharging current, polarization effects, and exponential voltage decay [9], [21]. The battery cell voltage during discharge is given by 9:

$$V_{disc} = V_0 - (\frac{K \cdot Q}{Q - Q_{act}})(Q_{act} + I^*) - R \cdot I + Ae^{-B \cdot Q_{act}}, \quad (9)$$

where V_{disc} is the battery voltage, V_0 is the battery constant voltage, Q is the battery capacity, Q_{act} is the battery actual capacity, R is the internal resistance, I is the battery current, I^* is the filtered current, A is the exponential zone amplitude, B is the exponential zone time constant inverse, and K is the polarization constant.

2) Charging Strategy: A constant-power to taper charging strategy is implemented to reflect realistic HEA charging constraints during sequential flight operations. The charging profile is defined as:

$$W_{ch} = \begin{cases} W_{max}, & \text{if } 20\% \leq SOC \leq 80\%, \\ W_{max} \times \frac{100 - SOC}{r}, & \text{if } 80\% < SOC \leq 100\%, \end{cases} \quad (10)$$

where r, the SOC taper coefficient, was set to 20. Fig. 4 illustrates the charging profile.

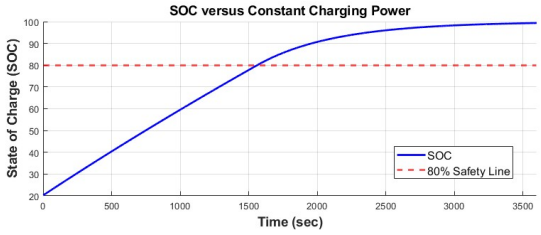

Fig. 4. Sample charging profile demonstrating constant power below 80% SOC, followed by a tapered regime to protect battery health.

III. Results

This section presents the sizing outcomes of the aircraft models, verifies the optimizer convergence, and compares airline sequence case studies from 2019 Mesa Airlines to evaluate HEA performance against a conventional baseline model of the ERJ175.

A. Model Design

Two aircraft models were developed based on the ERJ175LR top-level and mission performance requirements, as shown in Table III. The HEA battery is based on current battery technology and has a specific energy of 250 kWh/kg [22]. The propulsion system of the HEA model is sized based on sea-level static (SLS) takeoff conditions, where 10% of the required power is provided by the electric motor, with the gas turbine supplying the remaining 90%, with both operating at maximum power code. During climb, the gas turbine continues at its maximum continuous power while the EM's power code is reduced to 30%. Sensitivity studies indicated that a higher EM share at takeoff would result in an undersized GT for cruise performance, and a climb power code exceeding 30% would necessitate an impractically heavy battery. The resulting battery pack design, assuming a system voltage of 223V, is given in Table II.

TABLE III
Conventional (Conv.) and HEA TLARs and Specifications.

Group	Specification	Conv.	HEA
ERJ175LR TLARs and Specifications	Design Range (nmi)	2150	2150
	Max Passengers	78	78
	Thrust-to-Weight Ratio	0.339	0.339
	Cruise Mach	0.78	0.78
	Wing Loading (kg/m^2)	533.4	533.4
	Cruise L/D	15.2	15.2
	Max RC (m/s)	11.43	11.43
Sized Aircraft Parameters	MTOW (kg)	38,637	41,147
	Empty Weight (kg)	21,545	23,093
	Block Fuel (kg)	9,397	9,364
	Battery Weight (kg)	–	996.4
	Total SLS Thrust (kN)	123.4	131.5
	SLS Engine Thrust (kN)	61.7	59.2
	Wing Area (m^2)	72.4	77.2
	Avg Takeoff Engine TSFC [kg/(kN·h)]	39.12	31.92
	Avg Cruise Engine TSFC [kg/(kN·h)]	70.62	65.08
	EM Power (kW)	–	913.0
	Battery Energy (kWh)	–	249.1

B. Optimizer Verification

To verify the single-mission optimizer, a 1000 nmi off-design mission was used to assess whether fuel burn could be further reduced with adaptive power management while maintaining flight feasibility. A sensitivity study of varying input design variables confirmed that, within feasible bounds, the optimizer converged to the same optimal power management strategy (Table IV). Compared to an HEA using the original design power codes, the optimized HEA reduced fuel burn by 1.7%.

Fig. 5 depicts the climb power codes from the sized HEA model, which served as the initial design variables set as a function of climb altitude. The optimizer adjusted the GT and EM power codes while ensuring the GT could support the mission climb and the EM could operate between full throttle and off. Fig. 6 shows that the optimal solution adopts an on-off-on EM strategy, providing an additional boost at higher altitudes to expedite the climb and reach cruise more efficiently.

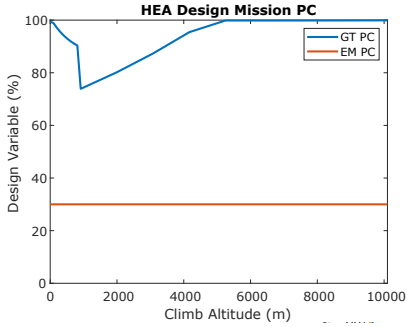

Fig. 5. Climb power codes from HEA model sized on design mission.

TABLE IV
INITIAL DESIGN VARIABLE CONVERGENCE SENSITIVITY STUDY.

Initial Design Variables (%)		Min Fuel	Battery Energy
EM PC	GT PC	Burn (kg)	Used (kWh)
Design PC	Design PC	3,800.96	195
100	100	3,800.96	195
50	100	3,800.96	195
0	100	3,800.96	195

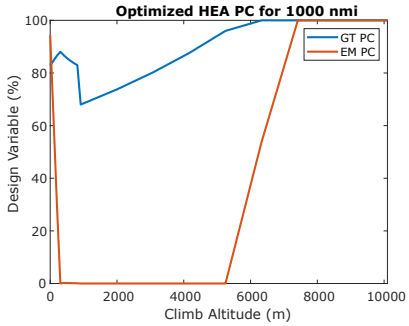

Fig. 6. Optimized climb power codes for a 1000 nmi mission.

C. Sequence Performance Comparison

The sequence in Table V was selected from Mesa Airlines January 2019 flight data to capture diverse mission lengths and limited turnaround times [9]. Specifically, the first two flights are both long, testing whether the battery can be recharged sufficiently between them given minimal ground time. The schedule then includes two shorter flights followed by another long flight, further highlighting how varying mission lengths and charging intervals affect overall performance. The first flight begins at 100% SOC to represent overnight charging, and each airport is assumed to have a 150 kW charger, a realistic assumption considering current DC fast-charging technology [23].

Four test cases were examined to evaluate power management strategies, optimizer performance, and HEA benefits over its conventional counterpart:

- *Case 1.* HEA with power codes optimized across the entire sequence using 3.
- *Case 2.* HEA with power codes optimized for each individual missions and inter-flight charging using 2.

TABLE V
SELECTED REGIONAL AIRLINE SEQUENCE TO TEST AIRCRAFT OPERATIONAL PERFORMANCE.

Flight	1	2	3	4	5
Origin	IAH	PHL	IAH	MEM	IAH
Destination	PHL	IAH	MEM	IAH	TUS
Distance (nmi)	1,151	1,151	406.7	406.7	813.4
Cruise Altitude (m)	10365	10365	9,144	9,144	10365
Time at Gate (min)	0	37	65	53	50

- *Case 3.* HEA using the original design power codes kept constant for all missions.
- *Case 4.* Conventional baseline model.

The total fuel burn and battery energy used for each case are reported in Table VI. Case 1 yields the lowest fuel burn and highest battery usage, while Case 3 saves only 1% fuel over the conventional baseline, highlighting the importance of optimized power management strategy for HEA operations.

TABLE VI
FUEL AND BATTERY ENERGY CONSUMPTION OF CASES ON TEST SEQUENCE.

Case	Total Fuel Burn (kg)	Fuel Burn % Diff wrt Case 4	Total Battery Energy Used (kWh)
Case 1	14,678	-2.99	636.1
Case 2	14,697	-2.87	635.3
Case 3	14,974	-1.04	556.6
Case 4	15,131	-	-

Fig. 7 compares the design variables and SOC profiles across the sequence. In Cases 1 and 2, the EM operates at full throttle early in the climb and again near the top of climb to support the GT, which experienced reduced power available at higher altitudes. Table VII summarizes the corresponding climb and flight times. In contrast, Case 3, which uses a constant 30% EM power, lacks sufficient top of climb boost, leading to a shallower, longer climb and higher total fuel burn. All HEA cases maintain a higher GT power code than the conventional baseline (Case 4). Although the HEA carries additional battery weight, the enhanced cruise efficiency of the smaller engine more than compensates for this penalty, resulting in lower overall fuel consumption.

TABLE VII
TIME TO CLIMB AND FLY THE MISSION FOR EACH FLIGHT IN EACH CASE, PRESENTED IN MINUTES AS: CLIMB TIME; FLIGHT TIME.

	Case 1	Case 2	Case 3	Case 4
Flight 1	20.9 ; 171	20.4 ; 171	23.0 ; 172	20.3 ; 171
Flight 2	21.1 ; 171	22.5 ; 171	23.0 ; 172	20.3 ; 171
Flight 3	16.3 ; 68.3	16.2 ; 68.3	16.9 ; 68.5	16.1 ; 68.1
Flight 4	16.3 ; 68.3	16.2 ; 68.3	20.6 ; 69.8	16.1 ; 69.0
Flight 5	19.7 ; 125	20.3 ; 125	21.8 ; 125	19.6 ; 124

Between the two optimized approaches, Case 1 achieves greater fuel savings by prioritizing an 80% SOC before each flight. In contrast, Case 2 fully depletes the battery (to 20% SOC) on the first flight, leaving insufficient ground time to recharge beyond 55% SOC for the second flight. Consequently,

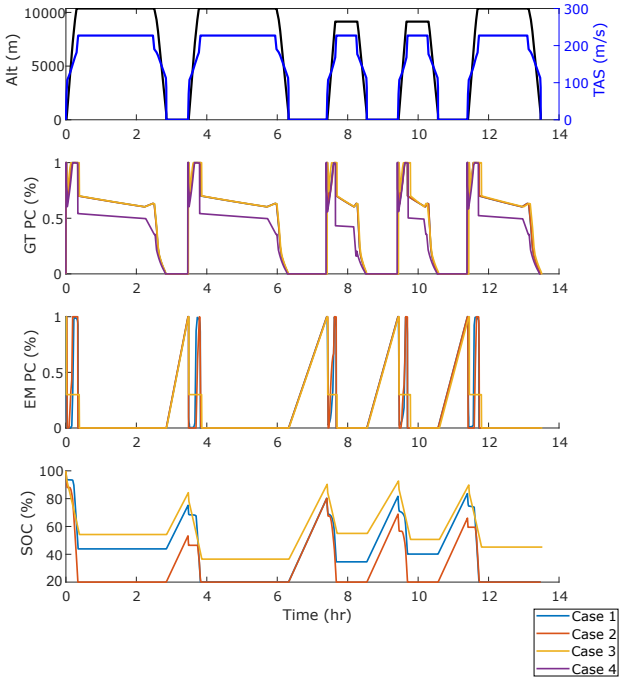

Fig. 7. Power codes and SOC for each case on the sequence.

the EM cannot provide as much support during subsequent climbs, leading to a higher overall fuel burn than Case 1.

D. Future Technology Comparison

Under current battery technology, the HEA incurs a significant weight penalty, limiting its fuel-burn advantage. To explore the impact of improved batteries, a new HEA model was sized for the same TLARs and design mission, with a 500 Wh/kg battery. The resulting advanced HEA is summarized in Table VIII.

TABLE VIII
ADVANCED HEA SIZED WITH 500 WH/KG BATTERY ASSUMPTION.

		% Change Over	
Specifications	**Value**	**Conventional**	**Current HEA**
MTOW (kg)	38,244	-1.02	-7.06
Empty Weight (kg)	21,065	-2.23	-8.78
Block Fuel(kg)	9,027	-3.94	-3.60
Battery Weight (kg)	458.0	-	-54.03
Total SLS Thrust (kN)	122.2	-0.97	-7.09
SLS Engine Thrust (kN)	55.0	-10.86	-7.09
Wing Area (m^2)	71.7	-0.97	-7.12
EM Power (kW)	848.5	-	-7.06
Battery Energy (kWh)	229.0	-	-8.03

When optimized over the same sequence with a high battery charging rate assumption of 500 kW, this advanced HEA reduced total fuel burn to 13,992 kg, which is -7.53% over Case 4 and -4.67% over Case 1, while using 892 kWh of battery energy. The power management of the optimized advanced and current technology HEA (Case 1) is compared in Fig. 8. The advanced HEA has an almost fully charged battery after every mission and uses higher electric motor power for longer during climb. This study shows that future technology levels will yield larger fuel burn reductions, and that power management optimization remains crucial to maximize the benefits because the mission profiles can vary widely. [24]

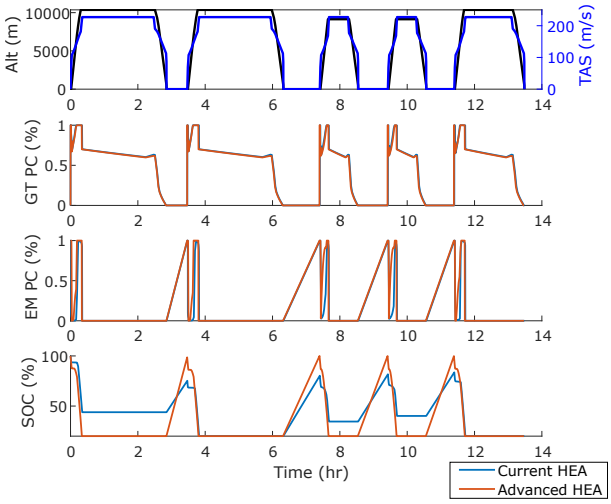

Fig. 8. Advanced and current HEA optimized power management over sequence.

IV. CONCLUSIONS

This study demonstrates that an adaptive power management strategy—one that dynamically allocates electric and gas turbine engine power across sequential flights—can achieve a 2–3% reduction in fuel burn compared to conventional configurations. By integrating aircraft sizing with realistic operational constraints, including limited gate charging durations and variable mission profiles, the proposed approach enhances overall propulsive efficiency despite the additional battery weight imposed by current technology. Improved engine modeling using the ICAO engine database further strengthens these findings by enabling more accurate predictions of climb and cruise performance.

The results indicate that HEA can be feasibly integrated into regional airline fleets without disrupting existing operations, provided that power management is optimized to balance energy depletion and battery state effectively. Moreover, even though the cruise phase does not operate in hybrid mode, the efficient operation of a downsized engine at higher throttle settings compensates for the battery weight penalty, yielding significant fuel savings during the dominant cruise segment.

Future work will extend this work to minimize operating cost while accounting for battery degradation and replacement costs. Such enhancements will further clarify the economic viability of HEA and support their adoption as a competitive alternative to conventional aircraft in regional operations.

ACKNOWLEDGMENTS

The authors thank Swapnil Jagtap, Yi-Chih Wang, and Paul Mokotoff for their contributions to this work; and Michael Ikeda for his role in the initial formulation of this research.

REFERENCES

[1] G. Cinar, Y. Cai, M. V. Bendarkar, A. I. Burrell, R. K. Denney, and D. N. Mavris, "System analysis and design space exploration of regional aircraft with electrified powertrains," *Journal of Aircraft*, vol. 60, no. 2, pp. 382–409, 2023. [Online]. Available: https://doi.org/10.2514/1.C036919

[2] M. Shi, G. Cinar, and D. N. Mavris, "Fleet analysis of a hybrid turboelectric commercial regional jet under nasa uli program," in *2021 AIAA/IEEE Electric Aircraft Technologies Symposium (EATS)*. IEEE, 2021, pp. 1–22.

[3] C. L. Pastra, C. Dull, R. Berumen, C. Yumuk, G. Cinar, and D. N. Mavris, "Viability study of an electrified regional turboprop," in *2022 IEEE Transportation Electrification Conference & Expo (ITEC)*. IEEE, 2022, pp. 231–236.

[4] H. Kühnelt, F. Mastropierro, N. Zhang, S. Toghyani, and U. Krewer, "Are batteries fit for hybrid-electric regional aircraft?" *Journal of Physics: Conference Series*, vol. 2526, no. 1, p. 012026, jun 2023. [Online]. Available: https://dx.doi.org/10.1088/1742-6596/2526/1/012026

[5] C. Pornet and A. Isikveren, "Conceptual design of hybrid-electric transport aircraft," *Progress in Aerospace Sciences*, vol. 79, pp. 114–135, 2015. [Online]. Available: https://www.sciencedirect.com/science/article/pii/S0376042115300130

[6] B. Chan, Y. Deng, N. Tran, H. Wu, M. Ikeda, G. Cinar, and M. Li, "Optimizing fleet assignment decisions for regional airlines with hybrid electric aircraft uptake." International Council of Aeronautical Sciences 2024, aug 2024. [Online]. Available: https://www.icas.org/ICAS_ARCHIVE/ICAS2024/data/papers/ICAS2024_0781_paper.pdf

[7] J. Hoelzen, Y. Liu, B. Bensmann, C. Winnefeld, A. Elham, J. Friedrichs, and R. Hanke-Rauschenbach, "Conceptual design of operation strategies for hybrid electric aircraft," *Energies*, vol. 11, no. 1, 2018. [Online]. Available: https://www.mdpi.com/1996-1073/11/1/217

[8] C. Lents, Z. Baig, and R. Taylor, "Parallel hybrid propulsion secondary power system architecture exploration and evaluation," in *2020 AIAA/IEEE Electric Aircraft Technologies Symposium (EATS)*, 2020, pp. 1–7.

[9] Y. Deng, A. Kryuchkov, P. Mokotoff, E. Smith, J. Patel, S. Garcia Lavanchy, M. Z. Li, and G. Cinar, "Operational Analysis for Hybrid Electric Aircraft Fleets: A feasibility study for the short- and medium-haul markets," in *AIAA AVIATION 2023 Forum*. San Diego, CA and Online: American Institute of Aeronautics and Astronautics, jun 2023. [Online]. Available: https://arc.aiaa.org/doi/10.2514/6.2023-3868

[10] Y. XIE, A. SAVVARISAL, A. TSOURDOS, D. ZHANG, and J. GU, "Review of hybrid electric powered aircraft, its conceptual design and energy management methodologies," vol. 34, no. 4, pp. 432–450. [Online]. Available: https://www.sciencedirect.com/science/article/pii/S1000936120303368

[11] M. Rendón, C. Sánchez, J. Gallo Muñoz, and A. Anzai, "Aircraft hybrid-electric propulsion: Development trends, challenges and opportunities (https://rdcu.be/cmg4u)," *Sba Controle Automação Sociedade Brasileira de Automatica*, 06 2021.

[12] G. Cinar, Y. Cai, R. K. Denney, and D. N. Mavris, "Modeling and simulation of a parallel hybrid electric regional aircraft for the Electrified Powertrain Flight Demonstration (EPFD) program," in *IEEE/AIAA Transportation Electrification Conference and Electric Aircraft Technologies Symposium*, 2022.

[13] P. Thantharate, A. Thantharate, and A. Kulkarni, "Greensky: A fair energy-aware optimization model for uavs in next-generation wireless networks," *Green Energy and Intelligent Transportation*, vol. 3, no. 1, p. 100130, 2024. [Online]. Available: https://www.sciencedirect.com/science/article/pii/S277315372300066X

[14] J. Hung and L. Gonzalez, "On parallel hybrid-electric propulsion system for unmanned aerial vehicles," *Progress in Aerospace Sciences*, vol. 51, pp. 1–17, 2012. [Online]. Available: https://www.sciencedirect.com/science/article/pii/S0376042112000097

[15] T. Kidd, Z. Yu, S. Dobbs, K. R. Anderson, G. Oetting, J. Kim, and M. O'Connell, "Uav power management, generation, and storage system principles and design," in *2020 IEEE Conference on Technologies for Sustainability (SusTech)*, 2020, pp. 1–8.

[16] P. Mokotoff, M. Arnson, Y.-C. Wang, and G. Cinar, "Fast: A future aircraft sizing tool for conventional and electrified aircraft design," in *AIAA SciTech 2025 Forum*, 2025, p. 2374.

[17] "14 cfr part 121 - operating requirements: Domestic, flag, and supplemental operations," *Code of Federal Regulations*, 2023, u.S. Federal Aviation Administration. [Online]. Available: https://www.ecfr.gov/current/title-14/chapter-I/subchapter-G/part-121

[18] *fmincon Documentation*. [Online]. Available: https://www.mathworks.com/help/optim/ug/fmincon.html

[19] J. Martins and A. Ning, *Engineering Design Optimization*, 10 2021.

[20] W. Industries, *Jet Refueler Spec Sheet*. [Online]. Available: https://superior.widen.net/s/lkgfqrjfrq

[21] O. Tremblay and L.-A. Dessaint, "Experimental validation of a battery dynamic model for ev applications," *World Electric Vehicle Journal*, vol. 3, no. 2, pp. 289–298, 2009. [Online]. Available: https://www.mdpi.com/2032-6653/3/2/289

[22] A. K. Koech, G. Mwandila, F. Mulolani, and P. Mwaanga, "Lithium-ion battery fundamentals and exploration of cathode materials: A review," *South African Journal of Chemical Engineering*, vol. 50, pp. 321–339, 2024. [Online]. Available: https://www.sciencedirect.com/science/article/pii/S1026918524001100

[23] U.S. Department of Transportation, "Charging speeds," Sep 2023, accessed: 2023-10-21. [Online]. Available: https://www.transportation.gov/rural/ev/toolkit/ev-basics/charging-speeds

[24] A. Kamat, B. Chan, A. Sharma, H. Wu, E. Cassidy, K. Kirsch, G. Cinar, and M. Z. Li, "Full airline network fleet assignment model with hybrid electric aircraft uptake," *IEEE Transportation Electrification Conference & Expo (ITEC)*, IEEE, Anaheim, CA, June 2025.